Unique Insights into PDAC Development Revealed by Both InSituPlex and Imaging Mass Cytometry

2021

Andrew A. Quong[1], Jordan Nieto[1], Derek Quong[1], Amanda Esch[1], Mael Manesse[2], Gourab Chatterjee[2], Devan Fleury[2], Keith A. Wharton Jr[2], Kirsteen H. Maclean[2], Mark Rees[2], Jeppe Thagaard[3], Fabian Schneider[3], Dan Winkowski[3], James Mansfield[3].

[1.] Fluidigm Corporation, 2 Tower Place, Suite 2000, South San Francisco, CA 94080; [2.] Ultivue 763D, Concord Ave, Cambridge, MA 02138; [3]Visiopharm, Agern Alle 24, 2970 Hørsholm, Denmark

Abstract

Pancreatic cancer remains a deadly disease due to difficulties hindering its early diagnosis, giving way to metastasis of the tumor and resulting in poor prognosis. While there are many neoplasms of the pancreas, pancreatic invasive ductal adenocarcinoma (PDAC) is the most common, and treatment options are few, with poor overall survival.

The complexities of the tumor microenvironment have been implicated in the failure of chemotherapy, radiation therapy, and immunotherapy. The tumor microenvironment of PDAC is especially rich with multiple interactions between pancreatic epithelial/cancer cells, stromal cells, immune cells, and the extracellular matrix (ECM). PDACs are characterized by a complex ECM of desmoplastic reaction consisting of an extensive and dense fibrotic stroma that surrounds and infiltrates clusters of malignant epithelial cells, together with the loss of basement membrane integrity and an abnormal vasculature.

In the present study we demonstrate a tissue phenotyping workflow combining three complementary methods that can unravel novel insights in the complex tumor microenvironment. This novel workflow delivers tissue morphology information, spatial phenotyping of immune cell population on whole slides, and high-dimensional imaging in selected regions of interest (ROIs) by combining H&E, multiplex immunofluorescence (mIF), and Imaging Mass Cytometry™ (IMC™).

Methods

A set of freshly serial sections from an FFPE block containing adenocarcinoma (PDAC) tissue sample was obtained commercially from Novus Biologicals. One section was stained using the protocols by Ultivue using the FixVUE I/O PD-L1 kit. The adjacent section was stained using the EpiMods panel from the Fluidigm Therapeutic Insights Services laboratory using the current Imaging Mass Cytometry Staining Protocol for FFPE Sections (Fluidigm PN 400322). The resulting images were reviewed by a pathologist, and multiple ROIs were selected based on PD-L1 expression and tumor morphology.

The images obtained using the FixVUE I/O kit were used to select the ROIs for ablation. The annotated images were imported in the instrument software (v7.0) and aligned with the slide stained for IMC acquisition, and the multiplexed data was acquired on the Hyperion™ Imaging System.

All digitized images were analyzed using the Visiopharm software platform (Hørsholm, Denmark). Regions of interest (Tumor, Stroma, and Blood Vessels) were automatically identified using thresholds after combining the Pan-CK + E-Cadherin channels to identify Tumor compartments, and the aSMA + Collagen-1 channels for identifying Stroma compartments and CD31 channel for identifying blood vessels. Magnification used for this task was 0.5X.

For detecting nuclei, a pre-trained Deep Learning algorithm available with the Visiopharm platform was used (U-Net architecture). To account for irregular morphology of macrophages, CD163 was included in the classification to improve the delineation of cells positive for that biomarker. Visiopharm's Multiplex Phenotyping module was used to automatically identify the range of biomarker combinations in the identified cells. The classification of each biomarker was semi-supervised and gated using two independently controlled parameters: signal intensity and percent coverage.

A second analysis pipeline starts with the raw MCD data, which is converted to an image stack. Data was pre-processed and image analysis stacks were generated using python. Image stack preprocessing was performed in CellProfiler™. The preprocessing steps included were hotspot removal and scaling the images by 2x for easier pixel classification.

For cell segmentation, an ilastik pixel classifier was trained using the ICSKs and DNA channels. All ROIs were labeled as either DNA, Cytoplasm/Plasma Membrane, or non-cellular. The outputs from this classifier were segmented in CellProfiler. First, the nuclei were segmented and used as seeds for the cell segmentation. Identified nuclei less then 2.5 microns (5 pixels after 2x scaling) in diameter were discarded. Cell boundaries were determined by propagating outwards from the nuclear seeds along the cytoplasm prediction.

Single-cell quantification (integrated intensities, mean intensities, etc.) was done in CellProfiler. Single-cell mean intensity data was normalized to the 99th percentile of all ROIs for each channel. For phenotyping cells, normalized mean intensities of non-negative and non-DNA/ICSK channels were included in a phenograph clustering, with k = 30

Results

Seven regions of interest (ROI) were identified for further analyses using the results from the Ultivue analysis. Two regions were labeled as high PD-L1, and the remaining expressed low to medium amounts of PD-L1.

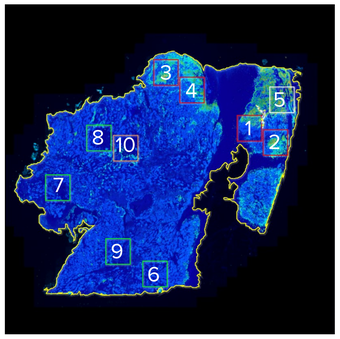

High PD-L1
ROIs 1, 2, 3, 4, 5

Moderate PD-L1
ROI 10

Low PD-L1
ROIs 6, 7, 8, 9

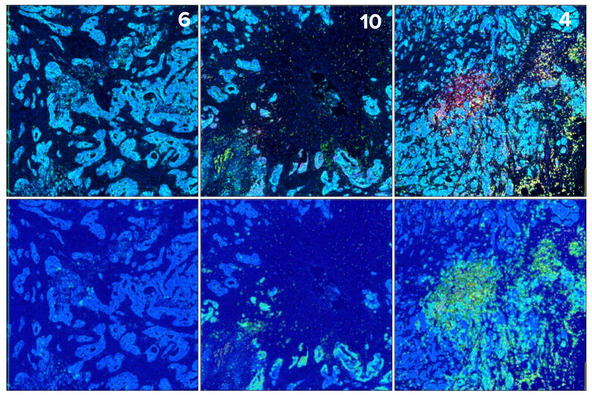

The top set of panels shows mIF using InSituPlex® CK/SOX10 (cyan), PD-L1 (red), and CD68 (green). Left to right: ROI 6 (PD-L1 low), 10 (PD-L1 moderate), and 4 (PD-L1 high).
The bottom set of panels is a heat map of PD-L1 expression density in the respective ROIs.

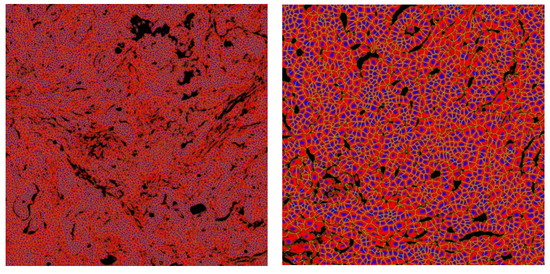

Pixel-based classification of cell segmentation when using both the Ir stain to identify nuclei and the ICSK markers (Pt194, Pt196, Pt198) to demark plasma membrane yields highly reproducible and excellent cellular delineation.

Results of the phenotyping using all the makers (without the ICSK panel) find 30 cell phenotypes distributed across the ROIs. As seen in the bar charts showing the distribution across the ROIs, there is a loss of group 0 in the low-to-medium PD-L1 ROIs and an increase in group 5 in the ROIs with high PD-L1 expression. As with the Visiopharm analysis, this loss of group 0 correlates with α-SMA cells and the co-expression of ECM proteins. The cells in group 5 represent cytotoxic cells including granulocytes and NK cells.

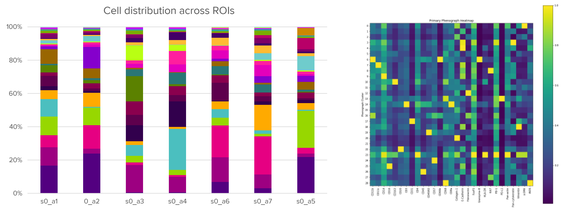

The distribution of cells is shown in two representative ROIs, low PD-L1 on the left and high PD-L1 on the right.

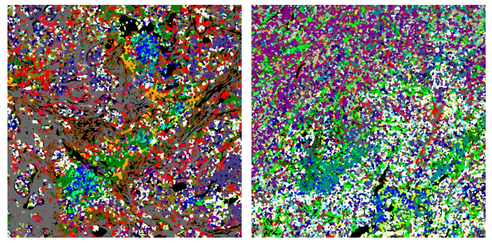

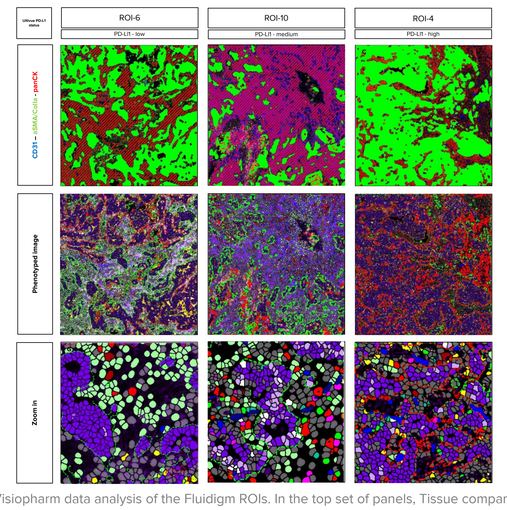

Visiopharm data analysis of the Fluidigm ROIs. In the top set of panels, Tissue compartments are deep-learning-based: stroma (green; α-SMA and Collagen I), tumor (red, pan-CK and E-Cadherin) and vessels (blue, CD31), and show a higher percentage of stroma across the low PD-L1 expressing ROIs. In the center panels, the distribution of the phenotyped cell types are shown for the 3 ROIs (ROI-6, -10 and -4).

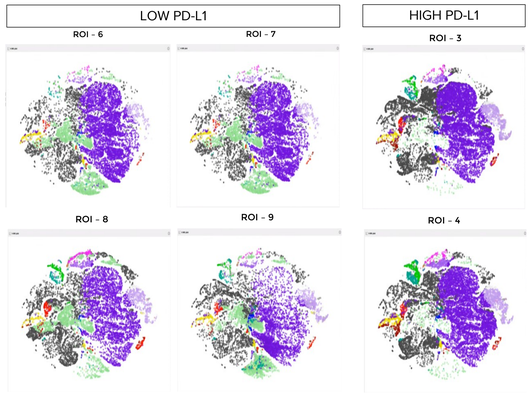

The t-SNE plots show the consistency of the cell distribution across the different ROIs with a similar PD-L1 expression and the marked difference between high and low expression.

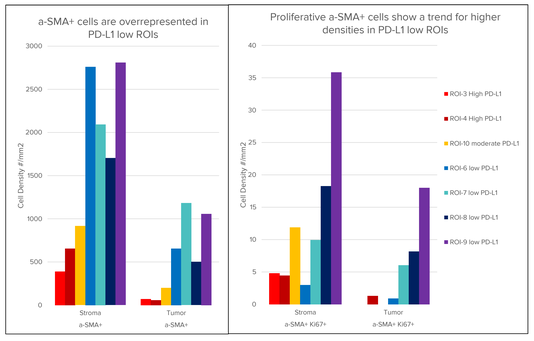

Low PD-L1 expressing ROIs (6 – 9) show a trend for higher stromal fibroblast (a-SMA+) and proliferative capacity of fibroblasts in these ROIs (a-SMA+ Ki67+) compared to high and moderate PD-L1 ROIs (1 – 5 and 10).

Summary

The combination of a whole-slide 8-plex mIF scan with image analysis to select regions of high/low PD-L1 content, along with 35-plex IMC imagery from these regions, coupled with deep-learning-based multiplex phenotyping image analysis, appears to allow for an interrogation of the tumor heterogeneity in PDAC. The use of the InSituPlex FixVUE I/O PD-L1 kit enabled the streamlined combination and alignment of whole-slide H&E and mIF data, leading to the strategic selection of regions of interest (ROIs) that represented very different regions of the tumor, while IMC technology enabled downstream imaging of 35 protein markers associated with the ECM in the selected ROIs to provide the basis for evaluation of the tumor microenvironment. Deeper cell profiling shows a correlation with low PD-L1 expression with increased Stroma, while areas with high PD-L1 expression show an increase in cells that express C11b, CD66, and Granzyme B.

Fluidigm Corporation,
2 Tower Place, Suite 2000, South San Francisco, CA 94080 USA
+1 650 266 6000 • Toll-free in the US and Canada: 866 359 4354
fluidigm.com

For Research Use Only. Not for use in diagnostic procedures.

References

1. Giesen, C., Wang, H.A.O. Schapiro, D., Zivanovic, N., Jacobs, A., Hattendorf, B., Schüffler, P.J., Grolimund, D., Buhmann, J.M., Brandt, S., Varga, Z., Wild, P.J., Günther, D., Bodenmiller, B. "Highly multiplexed imaging of tumor tissues with subcellular resolution by mass cytometry." *Noture Methods* (2014).
2. Chang, Q., Ornatsky, O., Siddiqui, I., Loboda, A., Baranov, V., Hedley, D.W. "Imaging Mass Cytometry." *Cytometry Part A* (2017).
3. Mavropoulos, A., Lin, D., Lam, B., Chang, T.K.J., Bisgrove, D., Ornatsky, O. "Equivalence of Imaging Mass Cytometry and immunofluorescence on FFPE tissue sections." fluidigm.com